DATA ANALYSIS REPORT

TOPIC:- **Multi-Scale Part-Based Syndrome Classification of 3D Facial Images**

NAME: CHANDANA M RAO

CLASS: 4CSE1

ROLL NO: 20221CSE007

SUBJECT CODE: CSE2027

ABSTRACT:

Identification and delineation of craniofacial characteristics support the clinical and molecular diagnosis of genetic syndromes. Deep learning (DL) frameworks for syndrome identification from 2D facial images are trained on large clinical datasets using standard convolutional neural networks for classification. In contrast, despite the increased availability of 3D scanners in clinical setups, similar frameworks remain absent for 3D facial photographs. The main challenges involve working with smaller datasets and the need for DL operations applicable to 3D geometric data. Therefore, to date, most 3D methods refrain from working across multiple syndromic groups and/or are solely based on traditional machine learning. The first contribution of this work is the use of geometric deep learning with spiral convolutions in a triplet-loss architecture. This geometric encoding (GE) learns a lower dimensional metric space from 3D facial data that is used as input to linear discriminant analysis (LDA) performing multiclass classification. Benchmarking is done against principal component analysis (PCA), a common technique in 3D facial shape analysis, and related work based on 65 distinct 3D facial landmarks as input to LDA. The second contribution of this work involves a part-based implementation to 3D facial shape analysis and multi-class syndrome classification, and this is applied to both GE and PCA. Based on 1,786 3D facial photographs of controls and individuals from 13 different syndrome classes, a five-fold cross-validation was used to investigate both contributions. Results indicate that GE performs better than PCA as input to LDA, and this especially so for more compact (lower dimensional) spaces. In addition, a part-based approach increases performance significantly for both GE and PCA, with a more significant improvement for the latter

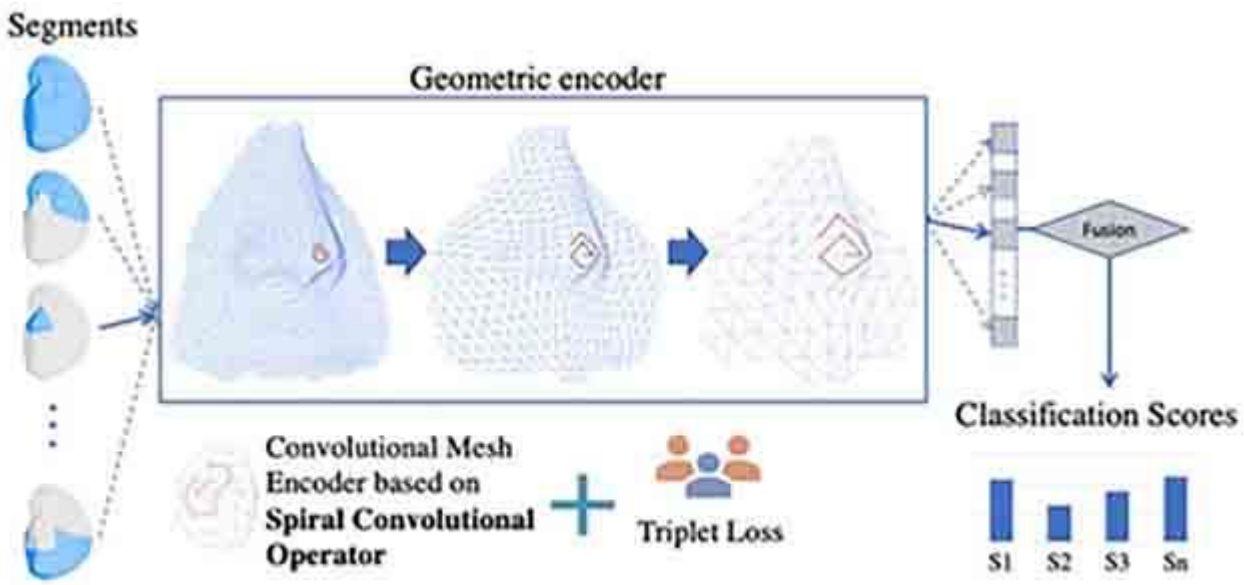

INTRODUCTION:

Date of Publication: **22 February 2022**

Published in: **IEEE Access (Volume: 10)**

Genetic conditions frequently present with distinct facial characteristics, which are often the first clue in diagnostics. To this day, a clinical diagnosis relies on an assessment by clinical experts who are trained to recognize facial phenotypes associated with syndroms. However, subtle facial phenotypes may not be obvious to the clinician. Further, it can be difficult for a clinician to keep pace with the ever-expanding catalog of clinical and molecular diagnoses and their associated phenotypes. Therefore, objective facial phenotyping for syndrome identification is needed to assist in clinical diagnosis . Previous work has mostly focused on 2D facial images , with large-scale deep convolutional neural networks being developed for and implemented in the clinic . While 2D photographs are easier to obtain, 3D images capture facial shape and morphology more directly and accurately as they are not subject to distortions due to projections, positional changes, and lighting conditions. Given the increasing accessibility of 3D imaging hardware, including consumer-grade depth sensors in modern smartphones , large-scale 3D shape analysis and deep learning for syndrome classification is becoming a practical possibility.

The main contributions of this work can be shortly listed as: 1) combining geometric deep learning with spiral convolutions and a triplet-based architecture, for the first time to learn phenotypic features that discriminate genetic syndromes from 3D facial shape; 2) incorporating a part-based approach to 3D facial shape analysis and multi-class syndrome classification such that the classification performance increases for both baseline and our geometric model; 3) providing visual and quantitative feedback on the classification output, and investigating the most distinguishing facial segment for classifying genetic syndromes by performing ablation studies within the part-based approach.

METHODOLOGY:

A. Dataset

The dataset comprises 1,786 3D facial images of controls and individuals clinically diagnosed into one of 13 different syndromes. All images were captured using the 3dMD or Vectra H1 3D imaging systems and were sourced from

B. Image Pre-Processing

To apply spiral convolutional operators, meshes with a fixed topology are required. This fixed topology also allows the removal of extraneous

$$P:R \rightarrow F$$

C. Learning Lower Dimensional Embeddings

1) Principal Component Analysis (PCA)
2) Geometric Encoder

$$\mathbf{h:F \rightarrow E, e=h(f)}$$

D. Full Pipeline

Starting from a raw image data r , the facial scan was pre-processed to generate the structured mesh representation:

$$1.f=P(r)$$

E. Training and Evaluation

1) Training
The GE blocks are trained for 600 epochs, when the validation loss plateaus, using the Adam optimizer, with a batch size of 60

2) Evaluation
To assess the non-linear metric learning based on a GDL architecture followed by LDA, we compared our results to those obtained using PCA followed by LDA as a baseline.

F. Experiments

1) Latent Space Dimensionality
2) Contribution of Part-Based Learning
3) One-Vs-All Geometric Encoder

RESULT:

A. Classification Performance Of Part-Based GE and PCA

The average balanced accuracy, sensitivity, specificity, and F1 score for each dimension are provided in Table 2. This table reports results of the full-face and the part-based models for both PCA and GE.

	BALANCED ACCURACY				SENSITIVITY / SPECIFICITY				F1 SCORE			
DIM	PCA FF	PCA PB	GE FF	GE PB	PCA FF	PCA PB	GE FF	GE PB	PCA FF	PCA PB	GE FF	GE PB
4	0.7 ± 0.047	0.82 ± 0.036	0.81 ± 0.037	0.87 ± 0.033	0.71 ± 0.092 0.69 ± 0.023	0.82 ± 0.075 0.83 ± 0.019	0.83 ± 0.071 0.78 ± 0.036	0.86 ± 0.066 0.88 ± 0.018	0.25 ± 0.03	0.42 ± 0.032	0.37 ± 0.04	0.5 ± 0.038
14	0.7 ± 0.038	0.82 ± 0.033	0.87 ± 0.035	0.87 ± 0.031	0.71 ± 0.079 0.69 ± 0.022	0.82 ± 0.072 0.83 ± 0.017	0.86 ± 0.066 0.88 ± 0.02	0.86 ± 0.063 0.88 ± 0.014	0.25 ± 0.032	0.42 ± 0.041	0.51 ± 0.049	0.5 ± 0.044
24	0.83 ± 0.037	0.89 ± 0.035	0.87 ± 0.036	0.88 ± 0.04	0.83 ± 0.075 0.84 ± 0.017	0.84 ± 0.07 0.94 ± 0.016	0.85 ± 0.072 0.89 ± 0.015	0.84 ± 0.082 0.93 ± 0.013	0.43 ± 0.035	0.63 ± 0.053	0.53 ± 0.041	0.61 ± 0.05
35	0.86 ± 0.029	0.88 ± 0.035	0.88 ± 0.028	0.88 ± 0.036	0.85 ± 0.062 0.87 ± 0.015	0.82 ± 0.068 0.94 ± 0.014	0.86 ± 0.06 0.9 ± 0.016	0.82 ± 0.073 0.94 ± 0.013	0.48 ± 0.031	0.64 ± 0.059	0.55 ± 0.039	0.62 ± 0.045
47	0.87 ± 0.031	0.88 ± 0.037	0.88 ± 0.036	0.87 ± 0.037	0.86 ± 0.065 0.89 ± 0.017	0.81 ± 0.073 0.95 ± 0.012	0.86 ± 0.068 0.91 ± 0.015	0.8 ± 0.076 0.94 ± 0.011	0.52 ± 0.036	0.65 ± 0.057	0.57 ± 0.047	0.63 ± 0.047
57	0.88 ± 0.033	0.87 ± 0.037	0.88 ± 0.039	0.87 ± 0.039	0.86 ± 0.067 0.9 ± 0.016	0.8 ± 0.075 0.95 ± 0.013	0.85 ± 0.08 0.91 ± 0.015	0.79 ± 0.078 0.95 ± 0.013	0.55 ± 0.039	0.65 ± 0.053	0.58 ± 0.046	0.64 ± 0.049

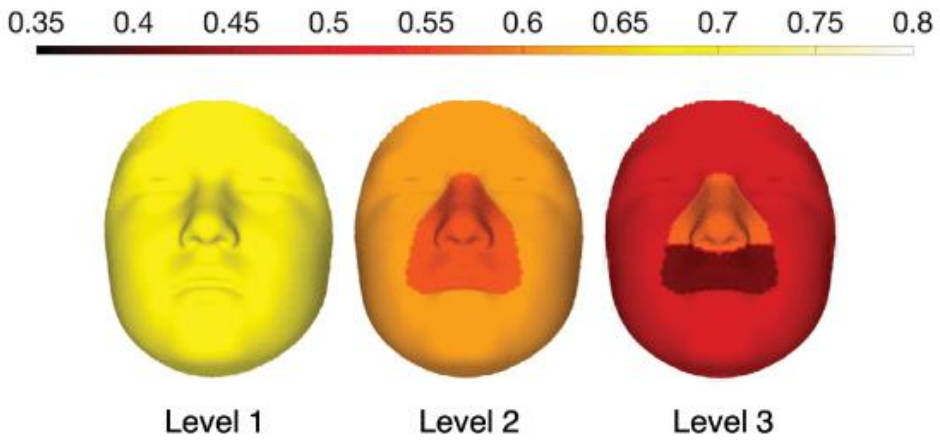

B. Classification Performance of Binary GE

Figure 6 shows the PR-AUC per syndrome obtained from each binary GE, multi-class GE, and PCA, all trained with a part-based setup with the optimal embedding dimension (24) per segment.

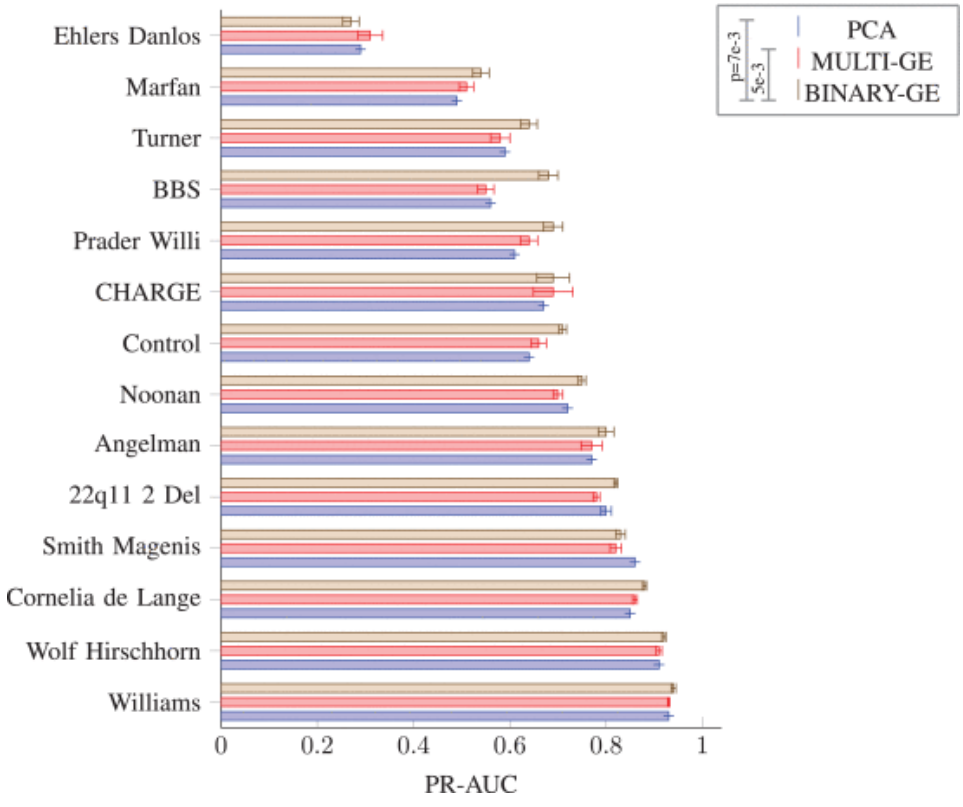

C. Influence of Individual Segments

Figure 7a displays the first two dimensions of a similarity space comparing the metric spaces derived from individual segments.

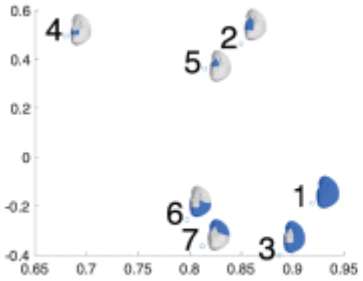

(a)

Removed segment	Fold 1	Fold 2	Fold 3	Fold 4	Fold 5	**Mean**	STD
/	0.652	0.629	0.688	0.635	0.664	**0.654**	0.0244
seg 1	0.525	0.568	0.567	0.572	0.588	**0.564**	0.0234
seg 2	0.397	0.396	0.38	0.354	0.407	**0.387**	0.021
seg 3	0.489	0.516	0.525	0.473	0.529	**0.506**	0.024
seg 4	0.279	0.245	0.255	0.276	0.287	**0.268**	0.018
seg 5	0.336	0.377	0.347	0.322	0.378	**0.352**	0.025
seg 6	0.345	0.317	0.341	0.325	0.352	**0.336**	0.015
seg 7	0.417	0.386	0.403	0.393	0.398	**0.399**	0.012

(b)

CONCLUSION:

In this work, we proposed a 3D part-based GDL model as an assisting tool for identifying candidate disorders based on facial shape from 3D surface images. First, we introduced a geometric encoder (GE) compared to PCA as input to LDA, where the former generated a clear improvement. Second, we proposed a part-based implementation to 3D facial shape analysis and multiclass syndrome classification, and this applied to both GE and PCA. The comparison between part-based versus holistic (or full face) approaches indicated substantial improvements. In addition, we are able to provide localized feedback on the contribution of each facial segment in the syndrome classification of a patient's image which aids clinicians in their assessment of the result. Lastly, based on ablation studies within the part-based approach, we investigated which facial segment stored the most unique information. This work is a collection of techniques found in the literature, and therefore, individual contributions to each of the components can further increase the work. To be more specific, future work includes optimizing the hierarchical facial segmentation using multi-task learning methods, instead of incorporating a previously obtained data-driven segmentation. Moreover, since many syndromes are extremely rare and hence their group size will always remain small, learning from highly imbalanced data techniques will become important. Lastly, other existing geometric deep learning methods, aside from the spiral convolutions used in this work, such as PointNet++ are of interest to explore since they enable learning from unstructured 3D data. However, a steeper learning curve is expected since extensive data normalization is less trivial to implement.

REFERENCES:

1.
Y. Gurovich, Y. Hanani, O. Bar, G. Nadav, N. Fleischer, D. Gelbman, et al., "Identifying facial phenotypes of genetic disorders using deep learning", *Nature Med.*, vol. 25, pp. 60-64, Jan. 2019.
Show in Context CrossRef Google Scholar
2.
Q. Ferry, J. Steinberg, C. Webber, D. R. FitzPatrick, C. P. Ponting, A. Zisserman, et al., "Diagnostically relevant facial gestalt information from ordinary photos", *eLife*, vol. 3, Jun. 2014.
Show in Context CrossRef Google Scholar
3.
B. Hallgrímsson et al., "Automated syndrome diagnosis by three-dimensional facial imaging", *Genet. Med.*, vol. 22, pp. 1682-1693, Oct. 2020.
Show in Context CrossRef Google Scholar
4.
D. L. Narayanan, P. Ranganath, S. Aggarwal, A. Dalal, S. R. Phadke and K. Mandal, "Computer-aided facial analysis in diagnosing dysmorphic syndromes in Indian children", *Indian Pediatrics*, vol. 56, no. 12, pp. 1017-1019, Dec. 2019.
Show in Context CrossRef Google Scholar
5.
J. T. Pantel, N. Hajjir, M. Danyel, J. Elsner, A. T. Abad-Perez, P. Hansen, et al., "Efficiency of computer-aided facial phenotyping (DeepGestalt) in individuals with and without a genetic syndrome: Diagnostic accuracy study", *J. Med. Internet Res.*, vol. 22, no. 10, Oct. 2020.
Show in Context CrossRef Google Scholar
6.
M. Quinto-Sánchez et al., "Developmental pathways inferred from modularity morphological integration and fluctuating asymmetry patterns in the human face", *Sci. Rep.*, vol. 8, no. 1, pp. 963-978, Dec. 2018.
Show in Context CrossRef Google Scholar